Lateral migration of a two-dimensional vesicle in unbounded Poiseuille flow

B. Kaoui,[1,2] G. H. Ristow,[3] I. Cantat,[4] C. Misbah,[1,*] and W. Zimmermann[3]
[1]*Laboratoire de Spectrométrie Physique, CNRS-Université Joseph Fourier, UMR 5588, BP 87, F-38402 Saint-Martin d'Hères Cedex, France*
[2]*Faculté des Sciences Ben M'Sik, Laboratoire de Physique de la Matière Condensée, Casablanca, Morocco*
[3]*Theoretische Physik, Universität Bayreuth, D-95440 Bayreuth, Germany*
[4]*Groupe Matière Condensée et Matériaux, Université de Rennes, 1, F-35042 Rennes Cedex, France*
(Received 25 June 2007; revised manuscript received 7 October 2007; published 5 February 2008)

The migration of a suspended vesicle in an unbounded Poiseuille flow is investigated numerically in the low Reynolds number limit. We consider the situation without viscosity contrast between the interior of the vesicle and the exterior. Using the boundary integral method we solve the corresponding hydrodynamic flow equations and track explicitly the vesicle dynamics in two dimensions. We find that the interplay between the nonlinear character of the Poiseuille flow and the vesicle deformation causes a cross-streamline migration of vesicles toward the center of the Poiseuille flow. This is in a marked contrast with a result [L. G. Leal, Annu. Rev. Fluid Mech. **12**, 435 (1980)] according to which the droplet moves away from the center (provided there is no viscosity contrast between the internal and the external fluids). The migration velocity is found to increase with the local capillary number (defined by the time scale of the vesicle relaxation toward its equilibrium shape times the local shear rate), but reaches a plateau above a certain value of the capillary number. This plateau value increases with the curvature of the parabolic flow profile. We present scaling laws for the migration velocity.

DOI: 10.1103/PhysRevE.77.021903 PACS number(s): 87.16.D−, 87.17.Jj, 87.19.rh

I. INTRODUCTION

Vesicles are closed phospholipid membranes suspended in an aqueous solution. They constitute a first step in a model aiming to capture elementary ingredients in the study of the dynamics of more complex entities such as red blood cells. Of particular interest is the migration of blood cells in the circulatory system. The study of migration of soft particles under flow presents fundamental (e.g., understanding the subtle interplay between deformation and the flow) as well as technological interests (e.g., understanding this problem may help monitoring vesicles and cell guidance in various circumstances, such as in microfluidic devices, in the process of cell sorting out, and so on).

In the present work we focus our attention on describing the dynamics of a single suspended vesicle in a nonlinear shear gradient of a plane Poiseuille flow. We consider the small Reynolds number limit, so that inertia can be neglected. Vesicles in flow field have been the subject of extensive studies, both in an unbounded linear shear flow [1–7,19] as well as in the presence of a wall [8–12]. In an unbounded linear shear flow (of low Reynolds number) a vesicle does not exhibit a lateral migration with respect to the flow direction. The presence of a wall breaks the translational symmetry perpendicular to the flow direction and a vesicle is found to migrate away from the wall [8–12]. This so-called lift force is caused by the flow induced upstream-downstream asymmetry of the vesicle [8]. More recently, it has been shown that even a spherical vesicle may execute a lift force as well, provided that the wall is flexible [13]. In that case, the wall deformability breaks the upstream-downstream symmetry.

A nonlinear shear flow has a nontranslationally invariant shear rate. It is therefore of great interest to understand its possible contribution to a cross-streamline migration process. Here we focus on the pure bulk effect due to the nonlinear shear gradient of a plane Poiseuille flow alone. Accordingly, we consider a parabolic flow profile in the absence of bounding walls (in order to avoid any wall induced lift force), and we consider neutrally buoyant vesicles so that gravity effect is suppressed.

We find that the curvature of the imposed velocity profile, together with the vesicle deformability, causes a systematic migration of a tank-treading vesicle perpendicularly to the parallel streamlines toward the flow center line. Our results show that the migration velocity increases with the curvature of the flow profile and we provide also scaling results for the migration velocity as a function of the local capillary number. This behavior is different from a prediction made for droplets [14], according to which droplets should migrate away from the center of the Poiseuille flow toward the periphery. Actually, in Ref. [14] it is predicted that the direction of the lateral migration of a droplet depends on the viscosity contrast. For values between 0.5 and 10, and particularly in the absence of a viscosity contrast as treated here, migration occurs toward the periphery, while for values smaller than 0.5 or greater than 10, it occurs toward the center line. We did not observe any of these scenarios neither from numerical studies, nor from our preliminary analytical results.

The scheme of this paper is as follows. In Sec. II we present the model equations and describe briefly the method used to solve the problem. In Sec. III we define the dimensionless parameters and provide typical experimental values. In Sec. IV numerical results and their discussion are presented. Section V is devoted to some concluding remarks.

*chaouqi.misbah@ujf-grenoble.fr

II. MODEL AND METHOD

A. Hydrodynamical equations and boundary integral method

The flow of an incompressible Newtonian fluid with viscosity η and density ρ is characterized by the dimensionless Reynolds number,

$$\mathrm{Re} = \frac{\rho V_0 R_0}{\eta}, \tag{1}$$

where V_0 is a characteristic velocity and R_0 is a characteristic length of the studied system. In our case we take the size of a vesicle, which is of the order of 10–100 μm [15], as the characteristic length. For such a length and for vesicles suspended in an aqueous solution subject to shear, with moderate applied shear rates ($\dot{\gamma}=V_0/R_0$) that are usually of the order of 10 s^{-1}, the Reynolds number is rather small, Re $\sim 10^{-2}-10^{-3} \ll 1$. Therefore, the flows of the fluids inside and outside the vesicle, which are taken to be of the same nature, are well approximated by the Stokes equations,

$$-\nabla p + \eta \nabla^2 \mathbf{v} = \mathbf{f},$$

$$\nabla \cdot \mathbf{v} = 0, \tag{2}$$

where $\mathbf{v}$ is the fluid velocity, p is the pressure, and $\mathbf{f}$ is the force imposed by the deformable vesicle membrane on the two fluids (it is a local force having a nonzero value only at the membrane). This force is given by the functional derivative of the vesicle membrane energy with respect to the membrane displacement, as discussed in the next section.

Using the boundary integral method [16,17] we solve Eqs. (2) in two-dimensional space. The velocity field at any point in the fluid (or at the membrane; the membrane velocity is equal to that of the adjacent fluids provided that the membrane is not permeable, and that there is no slip at the membrane) can be written as a superposition (due to linearity of the Stokes equations) of two terms, namely the contribution from the vesicle boundary, plus a contribution due to the undisturbed applied Poiseuille flow $\mathbf{v}(\mathbf{r})_{\mathrm{Pois}}$ (to be shown below),

$$v_i(\mathbf{r}) = \int_{\partial\Omega} d\mathbf{r}' \mathbf{G}_{ij}(\mathbf{r}-\mathbf{r}') f_j(\mathbf{r}') ds(\mathbf{r}') + v_i(\mathbf{r})_{\mathrm{Pois}}. \tag{3}$$

Here $\partial\Omega$ refers to the vesicle boundary. $\mathbf{G}_{ij}$ denotes the Oseen tensor, also called Green's function of the Stokes equations. Since we focus on dynamics of a vesicle suspended in an unbounded domain, we use the two-dimensional free space Green's function, that has the following expression [17,20]:

$$\mathbf{G}_{ij} = \frac{1}{4\pi\eta}\left(-\delta_{ij} \ln r + \frac{r_i r_j}{r^2}\right), \tag{4}$$

where $r \equiv |\mathbf{r}-\mathbf{r}'|$ and r_i is the ith component of the vector $\mathbf{r}-\mathbf{r}'$.

Equation (3) is valid in the fluid as well as at the membrane. In order to obtain the membrane velocity we replace $\mathbf{r}$ by the membrane vector position. Numerically, the vesicle membrane contour [in two dimensions (2D)] is discretized, as explained in Ref. [20]. After evaluating the membrane force which enters the right-hand side of Eq. (3) (see next section for the force evaluation), the velocity is then evaluated at each discretization point using Eq. (3). The displacement in the course of time of the vesicle membrane is obtained by updating the discretization points after each time iteration, using a Euler scheme, $\mathbf{r}(t+dt)=\mathbf{v}(\mathbf{r},t)dt+\mathbf{r}(t)$. In the following section we shall discuss in more detail the forces and the constraints.

B. Membrane force and comparison with droplets

The vesicle membrane is a bilayer made of phospholipid molecules having a hydrophilic head and two hydrophobic tails. At room temperature (and at physiological temperature as well) the membrane is fluid. The membrane can be viewed as a two-dimensional incompressible fluid. This incompressibility property implies the inextensibility of the membrane, and therefore, the conservation of local area. Moreover, since the vesicle encloses an incompressible fluid and the membrane permeability is very small, the vesicle volume must be a conserved quantity. Due to membrane impermeability, the membrane velocity is equal to the fluid velocity of the adjacent layer. Consequently, and because we use explicitly the incompressibility condition $\nabla \cdot \mathbf{v}=0$ for fluids, the enclosed volume is automatically conserved. The area of the membrane is not conserved automatically (think of a droplet that can spread out on a substrate; its volume is conserved while its surface increases). Thus, in order to fulfill membrane local area (or perimeter in 2D) conservation, one must introduce a surface (local) Lagrange multiplier. This Lagrange multiplier $\zeta(s,t)$ depends on the curvilinear coordinate s along the vesicle contour and on time, since the incompressibility should be fulfilled locally and at each time. ζ is the surface analog of the pressure field $p(\mathbf{r},t)$ which enforces local volume conservation of a three-dimensional (3D) fluid.

Due to the fact that phospholipidic molecules are bound to the membrane (there is no exchange between the bilayer and the surrounding solution), the local area (or area per molecule) remains constant in the course of time. This is a major difference with droplets, where the surface molecules can easily migrate into the underlying bulk and vice versa, causing thus a change of area. One may say that the surface molecules of a droplet are in contact with a large reservoir of molecules in the bulk (the reservoir fixes the chemical potential, while the number of molecules at the surface is a fluctuating quantity). For a droplet, the question of energy per unit surface makes sense: it corresponds to the increase in energy due to the transfer of a molecule from the bulk toward the surface. This is surface energy, or surface tension (note that for a liquid the surface energy and surface tension refer to the same quantity, while this is not the case for a solid). The surface force for a droplet is given by the classical Laplace law

$$\mathbf{f}_d = -\sigma H \mathbf{n}, \tag{5}$$

where σ is the surface tension, $\mathbf{n}$ is the outward normal unit vector, and H is the surface mean curvature. Note, that in the 2D case, as treated here, there is only one curvature H, and H is by convention counted to be positive for a circle.

As a vesicle membrane does not naturally change its area, the notion of cost of energy per unit area cannot be evoked. Moreover, one may think of changing the area by applying an external force and the surface energy is in this case the work associated with the applied force. This notion is, however, quite different from surface energy of a droplet. Here, for vesicles, we must rather refer to a surface stress, since by applying a force the intermolecular distance (due to stretching, for example) is modified. In contrast, a droplet may change its area without affecting the intermolecular distance. If we do not apply a large force in order to stretch the microstructure of the lipid layer, then membrane incompressibility is fulfilled. Hydrodynamical forces (as those encountered in this problem) are too small in comparison with cohesive forces, so that membrane incompressibility is safely satisfied.

From the mechanical point of view, the membrane can be viewed as a thin plate, where the soft (or easy) mode is the bending one. The corresponding energy is given by the Helfrich curvature energy [18]. This reads in 2D as

$$E_C = \frac{\kappa}{2}\int_{\partial\Omega} H^2 ds, \tag{6}$$

where κ is the membrane rigidity and H is the local membrane curvature. ds is the elementary arc length along the vesicle contour. Note that for the sake of simplicity, we do not account for a spontaneous curvature (a constant spontaneous curvature, H_0, may be included by substituting H by $H-H_0$). In order to take into account the area (perimeter in 2D) constraint, we must add to the above energy the following contribution $\int_{\partial\Omega}\zeta(s,t)ds$, so that the total energy reads

$$E = \frac{\kappa}{2}\int_{\partial\Omega} H^2 ds + \int_{\partial\Omega}\zeta(s,t)ds, \tag{7}$$

where $\zeta(s,t)$ is a local Lagrange multiplier. Note, that global conservation of the perimeter would be unphysical, because it would allow at some range of the membrane an arbitrarily large stretching and at the same time at another point a corresponding compression in a way that the global length is preserved. As discussed above, stretching or compression is possible only under the action of strong forces, of the order of cohesive forces.

The force acting on the membrane is obtained from the functional derivative of the vesicle energy E with respect to a membrane displacement. The resulting force has been already used previously (e.g., [8,20]), but a derivation has not been presented. A detailed derivation is given in the Appendix. The resulting force is

$$\mathbf{f} = \left[\kappa\left(\frac{\partial^2 H}{\partial s^2} + \frac{H^3}{2}\right) - H\zeta\right]\mathbf{n} + \frac{\partial\zeta}{\partial s}\mathbf{t}, \tag{8}$$

where $\mathbf{t}$ is the tangent vector (and recall that $\mathbf{n}$ is the normal vector). This force is composed of a normal as well as a tangential contribution. If ζ is constant, then only the normal part survives because of the following reason. If ζ is constant, the tensionlike force (which is a vector) associated with ζ is tangential to the curve, and has the same magnitude at both extremities of an arc element ds (which can be taken to be a portion of a circle, provided that ds is small enough). It follows, that the sum of the two forces is directed in the normal direction. If, on the contrary, ζ changes along the contour, then the two values at the extremities of ds are different, and the force has, besides a normal part, a tangential one, which is given by $(\partial\zeta/\partial s)\mathbf{t}$. On the other hand, the bending energy depends on the curvature (which is a geometrical quantity). It follows that the only force that is able to change the shape of a geometrical surface (i.e., a mathematical boundary having no internal physical structure) must be normal to the surface. Finally, note that the term $-\zeta H\mathbf{n}$ has the same structure as the force due to surface tension of a droplet equation (5). There is, however, a significant physical difference: for a droplet σ is an intrinsic quantity which represents the cost in energy for moving a molecule from the bulk (surrounded by other molecules) to the surface (and thus it loses some neighbors). In the present problem ζ is a Lagrange multiplier which must be determined *a posteriori* by requiring a constant local area. ζ is not an intrinsic quantity, but rather it depends on other parameters (such as κ, the vesicle radius, etc.).

C. Fulfilling local membrane area

In principle, from Eq. (3) we can determine the membrane velocity, if the force and the initial shape are given. The force (8) contains geometrical quantities (such as the normal and H) which are determined from the initial shape, plus a function $\zeta(s,t)$, which is unknown *a priori*. Numerically, the following method has been tested. An initial shape (typical of an ellipse) and an initial ζ (typical of a constant along the contour) have been chosen. Then the geometrical quantities appearing in the force can be calculated [the method of discretization of the integral Eq. (3) has been discussed in [20]]. This allows one to evaluate the right-hand side of (3) at initial time. The membrane velocity at this time is thus fixed. We then displace each membrane element according to the computed velocity, and by this way we obtain a new shape. However, the new shape does not fulfill, in general, the local membrane incompressibility. A local stretching (or compression) of the membrane takes place as long as the projected divergence of the velocity field of the fluid adjacent to the membrane is nonzero. We thus must adjust the appropriate function $\zeta(s)$ in order to fulfill this condition. The condition that the projected divergence must vanish reads as

$$(\mathbf{I}-\mathbf{nn}):\nabla\mathbf{v} = 0, \tag{9}$$

where $\mathbf{I}$ is the identity tensor, and $\mathbf{nn}$ stands for the tensor product ($\mathbf{I}-\mathbf{nn}$ is the projector on the contour). The above relation can be viewed as an implicit equation for $\zeta(s)$, similar to $\nabla\cdot\mathbf{v}=0$ which fixes the pressure field in 3D fluids. This way of reasoning is quite practical in the analytical study of vesicles [19]. From the numerical point of view, this way has suffered from several numerical instabilities. We have thus introduced another approach [20] as outlined below.

In a 2D simulation, when discretizing the vesicle membrane contour, the vesicle perimeter conservation constraint could be achieved without dealing with the local Lagrange

multiplier entering the membrane force given by Eq. (8). This constraint could be fulfilled in another and more convenient way. For that purpose we have used a straightforward method based on the fact that two material representative points on the membrane are attached to each other by strong cohesive forces which we describe by quasirigid springs, so that we can achieve in numerical studies less than 1% variation of the area. By this way an additional parameter k_s is introduced, which is the spring constant [20], $\zeta^N(i) = k_s[ds(i) - ds^0(i)]$. By choosing k_s large enough (in order to keep the membrane quasi-incompressible) the discretization step $ds(i)$ is kept as close as possible to its initial value $ds^0(i)$. Typically in units where $\eta = \kappa = 1$ and where the typical radius of vesicles is of order unity, a value of $k_s = 10^3$ has proven to be sufficient.

D. Applied flow

The applied Poiseuille flow $\mathbf{v}(\mathbf{r})_{\text{Pois}}$ has the following form:

$$\nu_x(\mathbf{r})_{\text{Pois}} = \nu_{\max}\left[1 - \left(\frac{y}{w}\right)^2\right],$$

$$\nu_y(\mathbf{r})_{\text{Pois}} = 0, \tag{10}$$

where $\nu_{\max}$ is the maximum velocity at the center line located at $y=0$ and $2w$ is the width of the Poiseuille profile. For our simulations we choose always the aspect ratio $R_0/w \ll 1$ in order to keep $\nu_x(w) = \nu_x(-w) = 0$ practically unperturbed by the presence of the vesicle.

III. DIMENSIONLESS NUMBERS

It is convenient to use in the simulation a dimensionless parameter that we call the local capillary number, which we define as

$$C_a(\mathbf{r}) = \tau\dot{\gamma}(\mathbf{r}). \tag{11}$$

τ is the characteristic time for a vesicle to relax to its equilibrium shape (in the absence of imposed flow), which is given by

$$\tau = \frac{\eta R_0^3}{\kappa}. \tag{12}$$

$\dot{\gamma}(\mathbf{r})$ is the local shear rate of the applied Poiseuille flow that can be evaluated from the corresponding velocity profile

$$\dot{\gamma}(\mathbf{r}) = \frac{\partial \nu_x(\mathbf{r})}{\partial y} = -\left(2\frac{\nu_{\max}}{w^2}\right)y = cy. \tag{13}$$

Here c is the curvature of the Poiseuille flow profile, which is given by $c = \partial^2\nu_x/\partial^2 y$. In the numerical scheme, there is another capillary number associated with the tension k_s (or spring constant), and is defined by $C_{as} = \dot{\gamma}\eta R_0/k_s$. In most simulations we have kept the ratio C_{as}/C_a small (of the order of 10^{-3}). This means that the time scale for stretching and/or compression of the membrane is fast in comparison to bending. In other words, local area conservation is adiabatically slaved to the overall shape evolution.

As a characteristic velocity we choose

$$V_0 = \frac{R_0}{\tau} = \frac{\kappa}{\eta R_0^2}, \tag{14}$$

with $R_0 \equiv L/2\pi$, where L is the vesicle perimeter. Hereafter we shall use τ as a unit of time, R_0 of length, and V_0 as unit of velocity. For typical experimental values of η (e.g., water), and by using standard values for vesicles $\kappa \sim 20k_BT$ (k_BT is the elementary thermal excitation energy) and $R_0 \sim 10$ μm one finds $\tau \sim 10$ s and $V_0 \sim 1$ μm/s. In the following (and especially in the figures of the simulation), when a velocity is written in terms of a number (without units) this means it is expressed in units of V_0. Since V_0 is typically of order 1 μm/s, the velocity is given practically in μm/s. The reported values for the velocities in experiments on vesicles are in the range of 1–100 μm/s [6,24]. In the circulatory system, data for the shear stress at the vessel wall are well documented [21]. For example, in arteries [21] the shear stress is of about 1–2 Pa. Dividing this by the plasma viscosity (close to that of water), one finds the shear rate at the wall, $\dot{\gamma}_{\text{wall}} \sim 10^3$ s^{-1}. The velocity at the center of the arteries is of about $\dot{\gamma}_{\text{wall}} w$. For small arteries $w \sim 100$ μm, so that $\nu_{\max} \sim 10^5$ μm/s (for venules, one has about $\nu_{\max} \sim 10^4$ μm/s). The chosen values in the simulations (see figures in the next section) are rather in the experimental range for vesicles, but are not far away from data on blood flow in arteries. Care must be taken however, since we have solved a 2D problem. Although we think that the orders of magnitudes should remain similar in 3D, further studies are needed before drawing conclusive answers.

IV. SIMULATION RESULTS AND DISCUSSION

Figure 1(a) illustrates a free vesicle in an unbounded plane Poiseuille flow, the dynamics of which is investigated. Figure 1(b) shows the time evolution of the lateral position of a vesicle which has been released initially from five different vertical positions, $y_0 = 0, 1, 2, 3, 4$. In most cases we have studied quasicircular vesicles placed in a Poiseuille flow characterized by $v_{\max} = 800$ and $w = 10$. In all situations treated so far, vesicles migrate to the center of the Poiseuille flow where no further lateral migration is observed. The position gives the distance from the center of the Poiseuille flow measured in units of the vesicle effective radius (as defined in the preceding section). All the curves are linear in a large range and deviations from this linear law occur only close to the center of the Poiseuille flow, in a range smaller than the vesicle size.

During the migration the vesicle shape undergoes deformations due to the hydrodynamic stresses imposed by the Poiseuille flow on the membrane. The vesicle is deformed and tilted until reaching a quasistationary orientation which is oblique with respect to the parallel streamlines. Figure 2 shows different vesicle shapes deformation occurring in our simulations during the migration, from an initially elliptical shape at the initial position $y_0 = 1$ shown in Fig. 2(a), to a

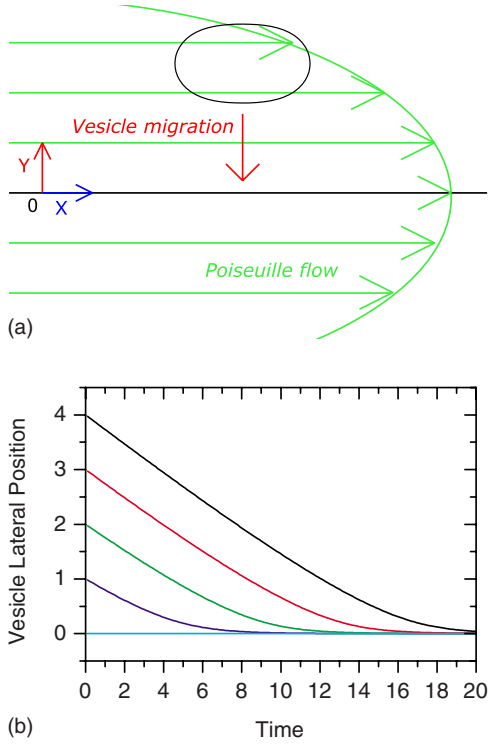

FIG. 1. (Color online) The plot (a) shows a schematic representation of the migration of a vesicle in a parabolic flow profile corresponding to an unbounded plane Poiseuille flow. The plot (b) shows the time evolution of the lateral position of a vesicle released initially at five different initial positions $y_0=0,1,2,3,4$ in units of the characteristic time τ (right-hand plot).

final parachute shape at the center of the Poiseuille flow as shown in Fig. 2(d). More or less similar parachute shapes are known for capsules and red blood cells [22,23] as they have been observed also experimentally for vesicles in Ref. [24], but all these examples concern capillary flows.

Before the vesicle reaches the center of the Poiseuille flow, it acquires an asymmetric shape as depicted in Fig. 2(b) and in Fig. 2(c). This asymmetry, which is caused by the nonuniform shear rate across the vesicle, is crucial for cross-streamline migration of vesicles in a plane Poiseuille flow.

As stated above, a drop (having no viscosity contrast with the ambient fluid) is predicted to drift toward the periphery [14]. Thus, vesicles and droplets behave quite differently. In Sec. II B we have presented the main differences between vesicles and droplets, both from the physical and the mathematical point of view. Which of these differences, albeit very important, may explain the differences in the migration direction, is not clear at present. For vesicles, we have explored a large domain of parameter space and in all cases the vesicle migrate toward the center. This result is also confirmed by preliminary analytical calculations in the quasi-spherical limit (following the spirit in Ref. [19]) in three spatial dimensions. This points to the fact that the migration direction does not depend on the dimensionality.

The migration velocity depends on various parameters. Of particular importance are the curvature of the velocity profile of the Poiseuille flow and the local capillary number, as discussed in the following. To the best of our knowledge, there is in the absence of a wall no lateral migration in a linear shear flow. In the presence of a flow with a nonlinear shear gradient, migration becomes possible, provided that the shear rate changes on the scale of the vesicle size. Therefore, curvature of the Poiseuille flow profile plays an essential role, but more precisely, the magnitude of the local capillary number, which determines essentially the vesicle deformation (which loses the up-down symmetry due to the shear gradient), is the most relevant quantity.

The dependence of the migration velocity on the local capillary is shown in Fig. 3 for different values of $v_{\max}$, w, and c, after the decay of an initial transient. In Fig. 3(a) and in Fig. 3(b) we kept the value of $v_{\max}$ fixed and we investigated the vesicle migration by varying the value of w. For smaller values of w, which corresponds to larger values of the curvature c, the vesicle migrates faster toward the center of the Poiseuille flow. Figure 3(b) shows the data collapse by plotting the migration velocity normalized to the curvature versus the local capillary number. In Fig. 3(c) and in Fig. 3(d) we kept w fixed and we examined the effect of varying the value of $v_{\max}$ for each value of w. The vesicle migrates faster with increasing values of $v_{\max}$ for every fixed w, because the curvature c increases with $v_{\max}$. Data collapse is again obtained in Fig. 3(d) by plotting the normalized migration velocity versus the local capillary number. The data collapse is more pronounced for smaller values of the curvature. In Fig. 3(e) and Fig. 3(f) we have varied $v_{\max}$ and w in such a way to keep the curvature fixed. We find that the vesicle migrates in this case to the Poiseuille flow center line for the three parameter combinations exactly (i.e., quantitatively the same results) in the same manner, which emphasizes again the important role of the nonlinear shear field. From the above study, we can conclude that the migration velocity in an unbounded Poiseuille flow normalized to the curvature c

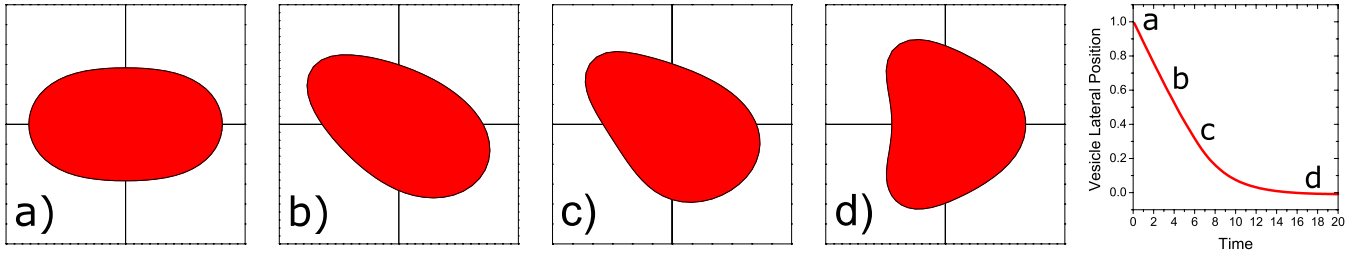

FIG. 2. (Color online) The shape of the vesicle changes from an initially elliptical shape in part (a) to the final parachute shape in (d) when it migrates toward Poiseuille flow center line, reduced area $\nu=0.90$.

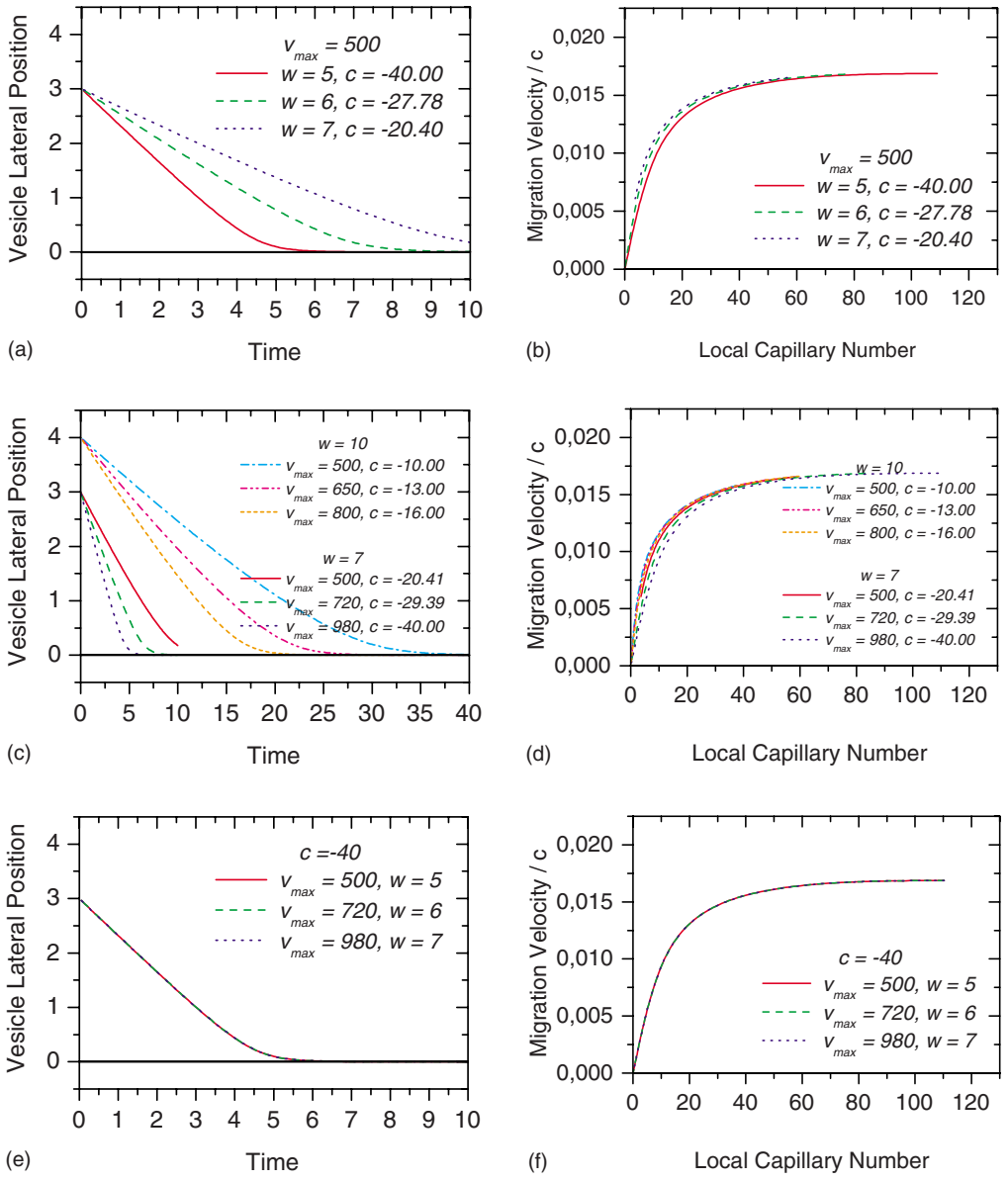

FIG. 3. (Color online) Time evolution of the vesicle position in an unbounded Poiseuille flow and its corresponding normalized migration velocity versus the local capillary number for different values of $v_{\max}$, w, and c (see text). The data correspond to the situation where initial transients have decayed.

should be described by the following universal scaling law:

$$\frac{v_{\text{migration}}(y)}{c} \sim f[C_a(y)]. \tag{15}$$

The extraction of this law is based on results of Figs. 3(b), 3(d), and 3(f). The function f is universal and depends only on C_a. The analytical form of the universal function is not known. A first step toward this issue is to develop an analytical theory in the small deformation limit, as in Ref. [19]. The small deformation limit provides us with nonlinear differential equations for the shapes and the migration of the vesicle instead of the less tractable integrodifferential equation (3). With this semianalytical approach, progress seems more likely for both, for an understanding of the migration direction, and the determination of the scaling function f. Related results will be presented elsewhere.

If the initial vesicle shape is not quasicircular but elliptical, we find a similar behavior as depicted in Fig. 3. The deformability of the vesicle, which depends on the bending rigidity κ, is a further ingredient for migration. This question is under investigation. It has been shown earlier that rigid spheres migrate only due to the contribution of $(v\cdot\nabla)v$ in the Navier-Stokes equation [25], which is beyond the Stokes limit. Similar trends as for a vesicle are obtained for deformable bead-spring models [26], where the migration velocity decreases with increasing rigidity of the tumbling object, corresponding also to increasing values of the spring constant. Indeed the vesicle deformability is, besides the nonlinear shear gradient, the main ingredient for the lateral migration in the Stokes limit. A vesicle in unbounded Poiseuille

flow undergoes large deformations ($C_a \gg 1$, see Fig. 3) caused only and mainly by the curvature of the velocity profile.

V. CONCLUSIONS

The dynamical behavior of a single vesicle placed in an unbounded plane Poiseuille flow has been investigated numerically. We found that the vesicle migrates during its tank-treading motion toward the center of a parabolic flow profile. The migration velocity is found to increase with the local capillary number (defined by the time scale of the vesicle relaxation toward its equilibrium shape times the local shear rate), but reaches a plateau above a certain value of the capillary number. This plateau value increases with the curvature of the parabolic flow profile c. When the vesicle reaches this final equilibrium position, its lateral migration velocity vanishes and it continues to move with a parachute shape parallel to the flow direction. We found that the migration velocity normalized to the curvature $v_{\text{migration}}/c$ follows essentially a universal law where the universal function depends on the local capillary number C_a, namely $v_{\text{migration}}/c \sim f(C_a)$. A droplet having no viscosity contrast seems to move away from the center [14], which is in a marked contrast to vesicles, for which we found migration toward the center. This difference is not yet fully understood, and is currently under investigation. Preliminary analytical results on the vesicle migration in three spatial dimension as well as on the migration velocity of bead- spring models in three spatial dimensions confirm our presented results on the migration vesicles in two spatial dimensions. This implies, in particular, that the dimensionality is not decisive for the migration tendency.

The present study has been concerned with a 2D problem. For example, the lift force close to a substrate was also studied in 2D in Ref. [8], and later the problem was solved in 3D [10]. It has been found that the basic features in 3D are similar to those captured in 2D simulations. More recently, the study of tank treading to tumbling transition has been analyzed numerically in 2D [3], and a systematic comparison with existing theories has been made. It has been found that the 2D and 3D results are both qualitatively and quantitatively very close to each other. The inclination angle in shear flow in 2D as a function of the excess area present rather reasonable agreement with experimental studies [7]. These various studies seem to point out that the 2D model captures essential features. It is nevertheless important to deal with the 3D question in the future.

Finally, in a forthcoming presentation our calculation will be also extended to droplets in order to extract the main source of difference between the vesicle and drop migration.

ACKNOWLEDGMENTS

The authors would like to thank A. Arend and S. Schuler for enlightening and very helpful discussions. One of the authors (C.M.) acknowledges financial support from CNES (Centre National d'Etudes Spatiales) and from CNRS (ACI Modélisation de la cellule et du myocarde). One of the authors (W.Z.) acknowledges financial support from DFG (German science foundation) via the priority program SPP 1164. Two of the authors (B.K., C.M.) acknowledge a Moroccan-French cooperation program (PAI Volubilis).

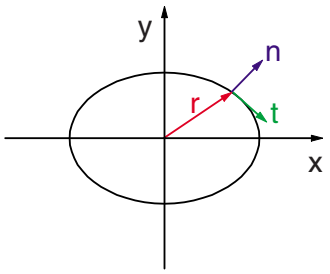

FIG. 4. (Color online) A schematic showing the vector position **r**, the normal **n**, and the tangent **t** unit vectors.

APPENDIX: DERIVATION OF THE MEMBRANE FORCE

In a two spatial dimension the vesicle membrane is represented by a one-dimensional closed contour. The corresponding membrane energy is an integral over this contour,

$$E = \frac{\kappa}{2}\int_0^L H^2(\mathbf{r})ds(\mathbf{r}) + \int_0^L \zeta(\mathbf{r})ds(\mathbf{r}), \tag{A1}$$

where L is the vesicle perimeter (i.e., the length of the contour) and $\mathbf{r}$ is the membrane vector position. Let,

$$E_C = \frac{\kappa}{2}\int_0^L H^2(\mathbf{r})ds(\mathbf{r}) \tag{A2}$$

and

$$E_T = \int_0^L \zeta(\mathbf{r})ds(\mathbf{r}). \tag{A3}$$

The counterclockwise tangent unit vector (see Fig. 4) is given by

$$\mathbf{t} = \frac{\partial \mathbf{r}}{\partial s}, \tag{A4}$$

and its derivative with respect to s defines the curvature,

$$\frac{\partial \mathbf{t}}{\partial s} = -H\mathbf{n}, \tag{A5}$$

where $\mathbf{n}$ is the outward unit vector normal to the curve. The derivative of $\mathbf{n}$ with respect to s gives

$$\frac{\partial \mathbf{n}}{\partial s} = H\mathbf{t}. \tag{A6}$$

Using Eq. (A4) and Eq. (A5) we get the expression of the curvature,

$$H^2 = \left(\frac{\partial^2 \mathbf{r}}{\partial s^2}\right)^2. \tag{A7}$$

The membrane force is deduced from the functional derivative of the energy $\delta E/\delta \mathbf{r}$, where $\delta \mathbf{r}$ is a local small displace-

ment of the vesicle membrane. Due to the displacement of $\mathbf{r}$ by $\delta\mathbf{r}$, ds will undergo variations as well. It is convenient to introduce a fixed parametrization (instead of s) of the curve, which is denoted by α. α is a parameter that we can take to vary from 0 to 1. The correspondence with s is such that $s(\alpha=0)=0$ and $s(\alpha=1)=L$. We then introduce the metric $g \equiv |\partial\mathbf{r}/\partial\alpha|^2$, so that $ds=\sqrt{g}d\alpha$. We convert the various terms in the energy by using now the variable α. The curvature assumes the following expression:

$$H^2 = \left[\frac{\partial^2\mathbf{r}}{\partial\alpha^2}\left(\frac{d\alpha}{ds}\right)^2 + \frac{\partial\mathbf{r}}{\partial\alpha}\frac{d^2\alpha}{ds^2}\right]^2, \tag{A8}$$

$$H^2 = \frac{1}{g^2}\left(\frac{\partial^2\mathbf{r}}{\partial\alpha^2} - \frac{\partial^2 s}{\partial\alpha^2}\mathbf{t}\right)^2. \tag{A9}$$

Writing $\partial^2\mathbf{r}/\partial\alpha^2$ in terms of the tangent and the normal vectors, it is straightforward to show that

$$\frac{\partial^2\mathbf{r}}{\partial\alpha^2} = \frac{d^2 s}{d\alpha^2}\mathbf{t} - gH\mathbf{n}, \tag{A10}$$

This allows to eliminate s from the expression for H,

$$H^2 = \frac{1}{g^2}\left[\left(\frac{\partial^2\mathbf{r}}{\partial\alpha^2}\right)^2 - \frac{1}{g}\left(\frac{\partial^2\mathbf{r}}{\partial\alpha^2}\frac{\partial\mathbf{r}}{\partial\alpha}\right)^2\right]. \tag{A11}$$

1. Curvature force

Replacing in Eq. (A2) H^2 by the expression given in Eq. (A11) we obtain

$$E_C = \frac{\kappa}{2}\int_0^1 \left(\ddot{\mathbf{r}}^2 - \frac{1}{g}(\ddot{\mathbf{r}}\dot{\mathbf{r}})^2\right) g^{-3/2} d\alpha. \tag{A12}$$

The functional derivative of E_C reads as (from classical variation results)

$$\frac{\delta E_C}{\delta\mathbf{r}} = \frac{\partial e_C}{\partial\mathbf{r}} - \frac{\partial}{\partial\alpha}\frac{\partial e_C}{\partial\dot{\mathbf{r}}} + \frac{\partial^2}{\partial\alpha^2}\frac{\partial e_C}{\partial\ddot{\mathbf{r}}}, \tag{A13}$$

with $e_C=(\kappa/2)\left[\ddot{\mathbf{r}}^2-\frac{1}{g}(\ddot{\mathbf{r}}\dot{\mathbf{r}})^2\right]g^{-3/2}$, $\dot{\mathbf{r}}=\partial\mathbf{r}/\partial\alpha$, and $\ddot{\mathbf{r}}=\partial^2\mathbf{r}/\partial\alpha^2$. Since e_C does not explicitly depend on $\mathbf{r}$, the first term on the right-hand side of Eq. (A13) vanishes. The second term gives

$$\frac{\partial}{\partial\alpha}\frac{\partial e_C}{\partial\dot{\mathbf{r}}} = \kappa\frac{\partial}{\partial\alpha}\left[-\frac{1}{g^{5/2}}\left((\ddot{\mathbf{r}}\dot{\mathbf{r}})\ddot{\mathbf{r}} + \frac{3}{2}(\ddot{\mathbf{r}})^2\dot{\mathbf{r}} - \frac{5}{2g}(\ddot{\mathbf{r}}\dot{\mathbf{r}})^2\dot{\mathbf{r}}\right)\right], \tag{A14}$$

$$\frac{\partial}{\partial\alpha}\frac{\partial e_C}{\partial\dot{\mathbf{r}}} = -\kappa\frac{\partial}{\partial\alpha}\left(-\frac{\partial^2 s}{\partial\alpha^2}\frac{H}{g}\mathbf{n} + \frac{3}{2}H^2\mathbf{t}\right), \tag{A15}$$

while the third one becomes

$$\frac{\partial^2}{\partial\alpha^2}\frac{\partial e_C}{\partial\ddot{\mathbf{r}}} = \kappa\frac{\partial^2}{\partial\alpha^2}\left(\frac{1}{g^{3/2}}\ddot{\mathbf{r}} - \frac{1}{g^{5/2}}(\ddot{\mathbf{r}}\dot{\mathbf{r}})\dot{\mathbf{r}}\right), \tag{A16}$$

$$\frac{\partial^2}{\partial\alpha^2}\frac{\partial e_C}{\partial\ddot{\mathbf{r}}} = \kappa\frac{\partial^2}{\partial\alpha^2}\left(-\frac{H}{\sqrt{g}}\mathbf{n}\right), \tag{A17}$$

$$\frac{\partial^2}{\partial\alpha^2}\frac{\partial e_C}{\partial\ddot{\mathbf{r}}} = \kappa\frac{\partial}{\partial\alpha}\left(-\frac{\partial(H\mathbf{n})}{\partial s} + \frac{\partial^2 s}{\partial\alpha^2}\frac{H}{g}\mathbf{n}\right). \tag{A18}$$

Reporting the above results into (A13), we obtain the following expression for the functional derivative:

$$\frac{\delta E_C}{\delta\mathbf{r}} = \kappa\frac{\partial}{\partial\alpha}\left(-\frac{\partial H}{\partial s}\mathbf{n} + \frac{1}{2}H^2\mathbf{t}\right), \tag{A19}$$

$$\frac{\delta E_C}{\delta\mathbf{r}} = -\sqrt{g}\kappa\left(\frac{\partial^2 H}{\partial s^2} + \frac{1}{2}H^3\right)\mathbf{n}. \tag{A20}$$

Therefore, the membrane curvature force is given by

$$\mathbf{f}_C = \kappa\left(\frac{\partial^2 H}{\partial s^2} + \frac{1}{2}H^3\right)\mathbf{n}, \tag{A21}$$

where the factor $\sqrt{g}$ disappears from the physical force, since this one must be defined as $\mathbf{f}_C=-(1/\sqrt{g})\delta E_C/\delta\mathbf{r}$, as explained at the end of this appendix.

2. Tension force

Finally Eq. (A3) takes the following form:

$$E_T = \int_0^1 \zeta(\mathbf{r})\sqrt{g}d\alpha, \tag{A22}$$

whose functional derivative is

$$\frac{\delta E_T}{\delta\mathbf{r}} = -\frac{\partial}{\partial\alpha}\frac{\partial e_T}{\partial\dot{\mathbf{r}}} \tag{A23}$$

with $e_T=\zeta(\mathbf{r})\sqrt{g}$. Note that e_T depends neither on $\mathbf{r}$ nor on $\ddot{\mathbf{r}}$. We easily find

$$\frac{\delta E_T}{\delta\mathbf{r}} = -\frac{\partial}{\partial\alpha}\left(\zeta(\mathbf{r})\frac{\dot{\mathbf{r}}}{\sqrt{g}}\right), \tag{A24}$$

$$\frac{\delta E_T}{\delta\mathbf{r}} = -\frac{\partial}{\partial\alpha}[\zeta(\mathbf{r})\mathbf{t}], \tag{A25}$$

$$\frac{\delta E_T}{\delta\mathbf{r}} = -\sqrt{g}\frac{\partial}{\partial s}[\zeta(\mathbf{r})\mathbf{t}], \tag{A26}$$

$$\frac{\delta E_T}{\delta\mathbf{r}} = -\sqrt{g}\left(\frac{\partial\zeta}{\partial s}\mathbf{t} - \zeta H\mathbf{n}\right). \tag{A27}$$

The membrane force associated with the Lagrange multiplier is then,

$$\mathbf{f}_T = -\left(\zeta H\mathbf{n} - \frac{\partial\zeta}{\partial s}\mathbf{t}\right). \tag{A28}$$

By adding Eqs. (A21) and (A28), we obtain the total membrane force,

$$\mathbf{f} = \left[\kappa\left(\frac{\partial^2 H}{\partial s^2} + \frac{H^3}{2} \right) - H\zeta \right]\mathbf{n} + \frac{\partial \zeta}{\partial s}\mathbf{t}. \tag{A29}$$

Let us briefly explain why the force is given by $\mathbf{f} = -(1/\sqrt{g})\delta E/\delta \mathbf{r}$ (and not just $-\delta E/\delta \mathbf{r}$). The reason is that what matters is a physical displacement of the curve element ds and not $d\alpha$ (which is a mathematical arbitrary parametrization). If one performs directly the variation on the integral, one finds (according to the previous results)

$$\delta E = -\int \left\{ \left[\kappa\left(\frac{\partial^2 H}{\partial s^2} + \frac{H^3}{2} \right) - H\zeta \right]\mathbf{n} + \frac{\partial \zeta}{\partial s}\mathbf{t} \right\} \sqrt{g} d\alpha \delta \mathbf{r}, \tag{A30}$$

$$\delta E = -\int \left\{ \left[\kappa\left(\frac{\partial^2 H}{\partial s^2} + \frac{H^3}{2} \right) - H\zeta \right]\mathbf{n} + \frac{\partial \zeta}{\partial s}\mathbf{t} \right\} ds \delta \mathbf{r} = -\int \mathbf{f} ds \delta \mathbf{r}. \tag{A31}$$

[1] M. Kraus, W. Wintz, U. Seifert, and R. Lipowsky, Phys. Rev. Lett. **77**, 3685 (1996).
[2] U. Seifert, Eur. Phys. J. B **8**, 405 (1999).
[3] J. Beaucourt, F. Rioual, T. Séon, T. Biben, and C. Misbah, Phys. Rev. E **69**, 011906 (2004).
[4] H. Noguchi and G. Gompper, Phys. Rev. Lett. **93**, 258102 (2004).
[5] K. H. de Haas, C. Blom, D. van den Ende, M. H. G. Duits, and J. Mellema, Phys. Rev. E **56**, 7132 (1997).
[6] M.-A. Mader, V. Vitkova, M. Abkarian, A. Viallat, and T. Podgorski, Eur. Phys. J. E **19**, 389 (2006).
[7] V. Kantsler and V. Steinberg, Phys. Rev. Lett. **95**, 258101 (2005); **96**, 036001 (2006).
[8] I. Cantat and C. Misbah, Phys. Rev. Lett. **83**, 880 (1999).
[9] U. Seifert, Phys. Rev. Lett. **83**, 876 (1999).
[10] S. Sukumaran and U. Seifert, Phys. Rev. E **64**, 011916 (2001).
[11] P. Olla, J. Phys. A **30**, 317 (1997).
[12] M. Abkarian, C. Lartigue, and A. Viallat, Phys. Rev. Lett. **88**, 068103 (2002).
[13] J. Beaucourt, T. Biben, and C. Misbah, Europhys. Lett. **67**, 676 (2004).
[14] L. G. Leal, Annu. Rev. Fluid Mech. **12**, 435 (1980).
[15] B. Alberts, A. Johnson, J. Lewis, M. Raff, K. Roberts, and P. Walter, *Molecular Biology of the Cell* (Garland, New York, 2001).
[16] O. A. Ladyzhenskaya, *The Mathematical Theory of Viscous Incompresible Flow*, 2nd ed. (Gordon and Breach, New York, 1969).
[17] C. Pozrikidis, *Boundary Integral and Singularity Mmethods for Linearized Viscous Flow* (Cambridge University Press, Cambridge, 1992).
[18] W. Helfrich, Z. Naturforsch. A **28c**, 693 (1973).
[19] C. Misbah, Phys. Rev. Lett. **96**, 028104 (2006); G. Danker, T. Biben, T. Podgorski, C. Verdier, and C. Misbah, Phys. Rev. E **76**, 041905 (2007).
[20] I. Cantat, K. Kassner, and C. Misbah, Eur. Phys. J. E **10**, 175 (2003); I. Cantat and C. Misbah, in *Transport and Structure in Biological and Chemical Systems, Lecture Notes in Physics*, edited by S. C. Müller, J. Parisi, and W. Zimmermann (Springer, Heidelberg, 1999), Vol. 532, pp. 93–136.
[21] See, for example, Y. C. Fung, *Biomechanics* (Springer, New York, 1990).
[22] C. Quéguiner and D. Barthès-Biesel, J. Fluid Mech. **348**, 349 (1997).
[23] T. W. Secomb, R. Skalak, N. Ozkaya, and J. F. Gross, J. Fluid Mech. **163**, 405 (1986).
[24] V. Vitkova, M. Mader, and T. Podgorski, Europhys. Lett. **68**, 398 (2004).
[25] J. Feng, H. H. Hu, and D. D. Joseph, J. Fluid Mech. **277**, 271 (1994).
[26] A. Arend, J. Leonhard, D. Kienle, and W. Zimmermann (unpublished).